

Influence of Ligand with Fine Difference at Donor Site on MMCT Property in Binuclear Mixed Valence Complexes^①

LI Su-Hua^{a, b, c} YANG Yu-Ying^{a, c} ZHANG Yu-Xiao^{a, c}
WU Xin-Tao^a SHENG Tian-Lu^{a②}

^a(State Key Laboratory of Structural Chemistry, Fujian Institute of Research on the Structure of Matter, Chinese Academy of Sciences, Fuzhou 350002, China)

^b(College of Chemistry, Fuzhou University, Fuzhou 350002, China)

^c(University of Chinese Academy of Sciences, Beijing 100049, China)

ABSTRACT To investigate how the electronic effect of ligand at donor site influences electronic communication or metal-to-metal charge transfer (MMCT) properties in similar mixed-valence (MV) complexes, a series of binuclear organometallic complexes, MeCp(dppe)RuCNFeCl₃ (**1**), MeCp(PPh₃)₂RuCNFeCl₃ (**2**), Cp*(dppe)FeCNFeCl₃ (**3**), Cp*(dppe)RuCNFeCl₃ (**4**) and Cp*(PPh₃)₂RuCNFeCl₃ (**5**), have been synthesized and characterized. The electronic absorptions of these complexes show the presence of MMCT properties between Ru^{II} or Fe^{II} and Fe^{III} ions, strongly supported by the theoretical calculations. With increasing electron-donating ability of ligands (PPh₃ > dppe, Cp* > MeCp) at donor site, the MMCT absorption bands are red-shifted, which expresses in the sequence of absorption bands with **1** (500 nm), **4** (536 nm), **2** (542 nm), **5** (580 nm) from high-energy to low-energy. Meanwhile, the MMCT absorption energy of **4** (536 nm) is larger than that of **3** (760 nm) due to the stronger electron-donating ability of Fe^{II} than Ru^{II}. Furthermore, these complexes belong to the Class II systems according to the Robin and Day's classification.

Keywords: metal-to-metal charge transfer (MMCT), mixed-valence complexes, Class II;

DOI: 10.14102/j.cnki.0254-5861.2011-2811

1 INTRODUCTION

Mixed-valence (MV) chemistry has attracted much interest of scientists over the past decades due to their distinctive magnetic^[1–6] and electrical properties^[7–12]. To investigate the intramolecular metal-to-metal charge transfer (MMCT) process between metals, a great number of MV complexes including the cyanide-bridged complexes have been synthesized as research models^[13–19]. At the same time, some theories have made breakthroughs^[20–24]. Based on the study of various complexes, scientists found that the degree of electronic communications of mixed-valence complexes is influenced by many factors, such as the orientation of cyanide bridges, the intrinsic property of metals or ligands, *cis/trans*-arrangements of molecular geometrical configuration, the external

temperature, solvent or salts and so on^[25–29]. The promotion of electronic communication of *trans*-arrangements is much easier than *cis*-arrangement for binuclear or trinuclear complexes^[19]. Also, it has been found that external temperature is one of the important factors affecting electron delocalization^[30]. Most recently, our group reported that the first example of tetra-nuclear Ru₂⁵⁺–CN–Ru₂⁵⁺ complex possesses MMCT properties due to the different spin states between the two Ru₂⁵⁺^[31]. To deeply understand the relationship between electronic communication or MMCT and molecular structures, it is necessary to further investigate the unsymmetrical binuclear compounds.

Herein, we report the syntheses, crystal structures and characterization of a series of complexes L₁L₂M^{II}–CN–Fe^{III}Cl₃ (L₁ = dppe or (PPh₃)₂, L₂ = MeCp or Cp*, M = Ru or

Received 16 March 2020; accepted 23 June 2020 (CCDC 1942653, 1942659, 1971831, 1971832 and 1971833 for **1**–**5**, respectively)

① We thank the National Science Foundation of China (21773243, 21973095) and the Strategic Priority Research Program of Chinese Academy of Sciences (XDB20010200) for financial support

② Corresponding author. Sheng Tian-Lu, E-mail: tsheng@fjirsm.ac.cn

Fe) to investigate how the electronic effect of ligand at donor site influences the electronic communication or MMCT properties. The tiny difference between dppe and (pPh₃)₂ ligands is that the former has one ethyl group while the latter contains two phenyl groups. Combined the characterization results and the theoretical calculation, these complexes are classified into the Class II system. Besides, it is found that the more rich-electron ligand or stronger electron-donating metal at donor site favors to promote intramolecular electron transfer between metals by comparing all these complexes.

2 EXPERIMENTAL

2.1 Physical measurements

The elemental analyses (C, H and N) were measured using Vario MICRO elemental analyzer. The Infrared (IR) spectra characterization was carried out on a Vertex 70 FT-IR spectrophotometer with KBr pellets. The electronic absorption spectra were measured in dichloromethane solution with the PerkinElmer Lambda 950 UV-Vis-NIR spectrophotometer. The single-crystal X-ray diffraction data for the complexes were collected on a Saturn724+ CCD diffractometer equipped with graphite monochromatic Mo-K α (λ = 0.71073 Å) radiation by using an ω -scan model technique at 293 K. All crystallographic structures were solved by direct methods using SHELXL-2014^[32, 33] and refined with Olex-2^[34] program package.

2.2 Materials and synthesis

2.2.1 Materials

All operations were conducted under an argon atmosphere using the standard Schlenk techniques unless other statements. The complexes of MeCp(dppe)RuCN^[35], (dppe = bis(diphenylphosphino)ethane, MeCp = methyl-cyclopentadienyl, Cp* = pentamethyl-cyclopentadienyl) MeCp(PPh₃)₂RuCN^[35], Cp*Fe(dppe)CN^[36], Cp*Ru(dppe)CN^[37, 38] and Cp*(PPh₃)₂RuCN^[39] were prepared according to the previous paper.

2.2.2 Synthesis

2.2.2.1 General procedure for the synthesis of M–CN–FeCl₃

L₁L₂M–CN (0.15 g) was mixed with 1.1 equiv. of FeCl₃ in 20 mL CH₃OH and the reaction was refluxed for 3 h. The resulting solution was concentrated, filtered, and recrystallized by diffusing n-hexane into the CH₂Cl₂ solution at room temperature, yielding crystal for single-crystal X-ray crystallography.

2.2.2.2 MeCp(dppe)RuCNFeCl₃ (1)

Yield 0.14 g (74.3%). Elemental analysis calcd. (%): C, 51.69; H, 4.07; N, 1.83. Found: C, 51.71; H, 4.04; N, 1.76. IR (KBr, cm⁻¹): 2000 (C≡N).

2.2.2.3 MeCp(PPh₃)₂RuCNFeCl₃ (2)

Yield 0.15 g (84.0 %). Elemental analysis calcd. (%): C, 56.99; H, 4.07; N, 1.53. Found: C, 57.05; H, 4.14; N, 1.55. IR (KBr, cm⁻¹): 2007 (C≡N).

2.2.2.4 Cp*(dppe)FeCNFeCl₃ (3)

Yield 0.13 g (72%). Elemental analysis calcd. (%): C, 57.14; H, 5.05; N, 1.80. Found: C, 56.97; H, 5.01; N, 1.70. IR (KBr, cm⁻¹): 1969 (C≡N).

2.2.2.5 Cp*(dppe)RuCNFeCl₃ (4)

Yield 0.13 g (70%). Elemental analysis calcd. (%): C, 50.27; H, 4.55; N, 1.54. Found: C, 50.45; H, 4.77; N, 1.63. IR (KBr, cm⁻¹): 1989 (C≡N).

2.2.2.6 Cp*(PPh₃)₂RuCNFeCl₃ (5)

Yield 0.12 g (64.6%). Elemental analysis calcd. (%): C, 59.43; H, 4.74; N, 1.48. Found: C, 58.99; H, 4.71; N, 1.42. IR (KBr, cm⁻¹): 1989 (C≡N).

3 RESULTS

3.1 X-ray structure determination

The crystallographic structures of complexes **1**~**5** are determined by single-crystal X-ray analysis at room temperature. Because of their similar structures, molecular structure of complex **1** is shown in Fig. 1 and other structures are shown in Fig. S1 in the Supporting Information. The space groups are *Cc*, *P2₁/n*, *C2/c*, *P2₁/n* and *P1̄* for complexes **1**~**5**, respectively. All crystal structures are composed of two moieties, FeCl₃ and L₁L₂M–CN (M = Fe or Ru; L₁ = Cp* or MeCp; L₂ = dppe or (PPh₃)₂). For complex **1**, Ru is coordinated by three C atoms from MeCp, two P atoms from dppe and one C atom of the cyanide group while Fe is connected to three Cl atoms and one N atom of the cyanide group. Table 1 shows the selected bond lengths and angles of all complexes, and the crystal data and structure refinement for complexes **1**~**5** are given in Tables S1 and S2 in the Supporting Information. The Ru^{II}/Fe^{II}–CN–Fe^{III} of these complexes is linear, and their angle of both Fe(Ru)–C≡N and Fe–N≡C is larger than 165°. The radius of Ru^{II} is larger than that of Fe^{II} since the bond lengths of Ru–P (2.283~2.349 Å) are longer than those of Fe–P (2.212 Å). With the increasing electron density at donor site, the Ru–P bond length elongates systematically with the sequence of 2.283 Å in **1**, 2.307 Å in **4**,

2.319 Å in **2** and 2.349 Å in **5**, respectively. Besides, the similar trend also occurs in Fe–N bond length. This indicates

that the (PPh₃)₂ ligand has a greater electron-donating ability than the dppe ligand.

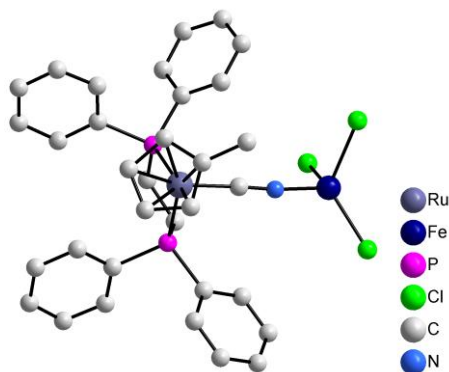


Fig. 1. Molecular structure of complex **1** (Hydrogen atoms in complex are ignored for clarity). Fe, red; C, gray; P, brown; Cl, green; N, blue

Table 1. Selected Bond Lengths (Å) and Bond Angles (°) of these Complexes

Complexes	1	2	3	4	5
C–N	1.168(7)	1.154(5)	1.176(5)	1.166(3)	1.163(6)
Fe(Ru)–C	1.930(6)	1.929(3)	1.814(4)	1.926(2)	1.919(4)
Fe–N	1.897(5)	1.929(3)	1.906(3)	1.922(2)	2.181(2)
Fe(Ru)–P(av.)	2.283(14)	2.319(9)	2.212(12)	2.307(7)	2.349(11)
Fe–Cl (av.)	2.155(13)	2.177(17)	2.187(17)	2.174(12)	2.179(4)
Fe(Ru)–C≡N	176.6(5)	174.4(3)	174.2(4)	172.7(2)	174.1(4)
Fe–N≡C	166.7(5)	177.1(3)	167.4(4)	170.7(2)	176.5(4)

3.2 IR spectroscopy

The IR spectroscopy test was conducted to characterize the vibrational frequency of the cyanide group. The data are listed in the experimental section and Table 2, which obviously shows that the stretching frequencies of these complexes are at least 50 cm^{−1} lower than those of their related precursors. There are two main reasons for the change of $\nu(\text{CN})$: one is the strong withdrawing-electron ability of FeCl₃ moiety pulling electron into cyanide group from the other fragment, which strengthens π back-bonding and hence makes the stretching of CN[−] red-shift^[40, 41]; and the other is the restrictions on cyanide group upon bonding to FeCl₃ fragment, which causes $\nu(\text{CN})$ blue-shift^[42]. For these complexes, the former reason is more important, so the CN stretching presents a red-shift. This change also suggests upon bonding with the strong acceptor unit FeCl₃, electron interaction between metals exists through the cyanide-bridged group. Owing to the increasing electron-rich properties from Cp*, MeCp, to Cp, the sequence of $\nu(\text{CN})$ from low to high energy is the Cp*Ru series (1989, 1989 cm^{−1}) < the MeCpRu series (2000, 2007 cm^{−1}) < the CpRu series (2003, 2013 cm^{−1}). Besides, Fe^{II} possesses a stronger electron-donating ability than Ru^{II}, which causes that the frequency of $\nu(\text{CN})$ in

complex **3** (1969 cm^{−1}) is lower than that of **4** (1989 cm^{−1})^[42]. It is interesting that $\nu(\text{CN})$ of complex **1** (Cc) shifts to lower frequencies than that of complex **2** (P2₁/n), which is not consistent with the previous papers. The same phenomenon occurs in complex Cp(dppe)RuCNFeCl₃ (Cc) and Cp(PPh₃)₂RuCNFeCl₃ (P2₁/n). Except the nature of ligands, the crystal configuration (space group) might be taken account as a major factor affecting the stretching of cyanide group.

3.3 UV-Vis-NIR spectroscopy

The data of maximum absorption band are listed in Table 3, and Fig. 2 exhibits the absorption bands of the mixed valence compounds and their relative precursors, which were conducted in the CH₂Cl₂ solution at room temperature. These bands of all complexes below 500 nm belong to the $d\pi(\text{Ru/Fe}) \rightarrow \pi^*$ metal to ligand charge transfer (MLCT) transitions^[4]. The absorption bands, up to 500 nm in the NIR region, are attributed to MMCT (metal to metal charge transfer), where electrons transfer from the CpRu/Fe to FeCl₃ moiety^[16, 42–44]. The MMCT band positions are in line with the results of theoretical calculations (Table 3), with the sequence of **1**(500 nm), **4**(536 nm), **2**(542 nm) and **5**(580 nm) from low- to high-wavelength. From Table 3, it can be found that

the position of absorption bands is proportional to the spin densities at donor site. As electron density of L_1L_2M increases, the absorption bands present a red-shift. Specially, the MMCT absorption energy of **4** (536 nm) is larger than that of **3** (760 nm), which is attributed to the stronger electron-donating ability of Fe^{II} than Ru^{II} . It's worth mentioning that there exist

two strong and broad absorption bands of compounds **1** and **4** due to the spin-orbit splitting of excited state configuration of low spin Fe^{III} , which generates three MMCT, as shown in Fig. 3^[17, 22, 45]. Owing to the small energy difference between spin-orbitals, only two overlapping absorption bands are experimentally observed.

Table 2. IR Spectra Bands, $\nu(CN)$ of Complexes 1~5 and Their Related Precursors (in KBr, cm^{-1})

Complexes	$\nu(CN)$	Related precursors	$\nu(CN)$	$\Delta\nu$
1	2000	MeCp(dppe)RuCN	2071	-71
2	2007	MeCp(PPh ₃) ₂ RuCN	2061	-54
3	1969	Cp*(dppe)FeCN	2054	-85
4	1989	Cp*(dppe)RuCN	2068	-79
5	1989	Cp*(PPh ₃) ₂ RuCN	2066	-77

Table 3. Comparison of Experimental and Theoretical Values of Electronic Absorption Bands in CH_2Cl_2 Solution

Complexes	$\lambda_{max} (\epsilon_{max})$ (nm ($M^{-1} cm^{-1}$))	
	Exptl.	Calcd.
1	500 (4391)	519.90
2	542 (4865)	546.86
3	760 (4378)	863.00
4	536 (3467)	534.15
5	580 (4344)	564.76

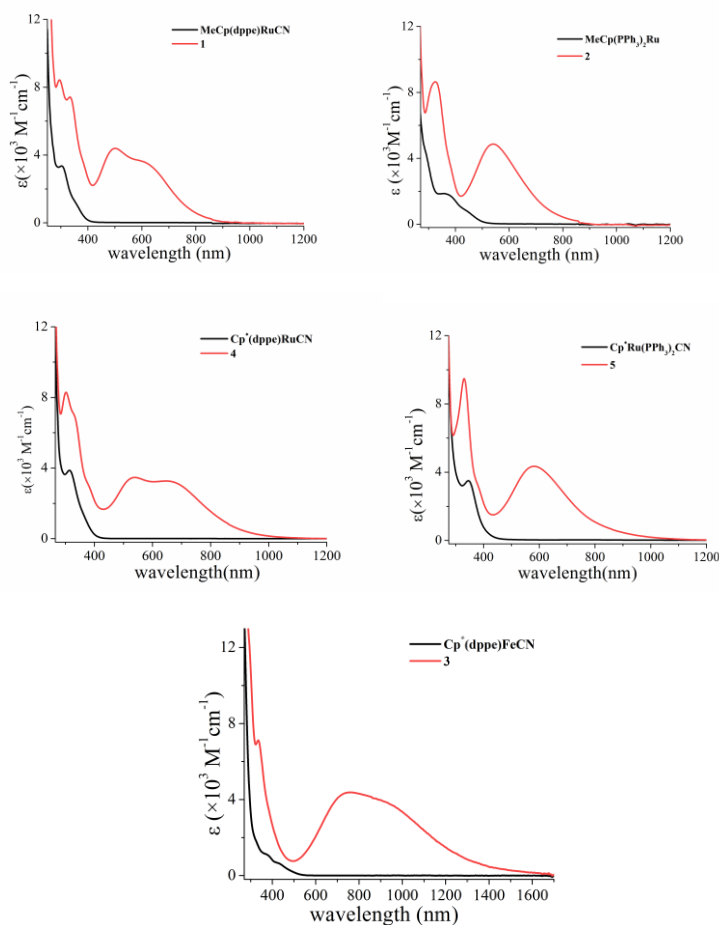


Fig. 2. UV-VIS-NIR absorption spectra of all complexes

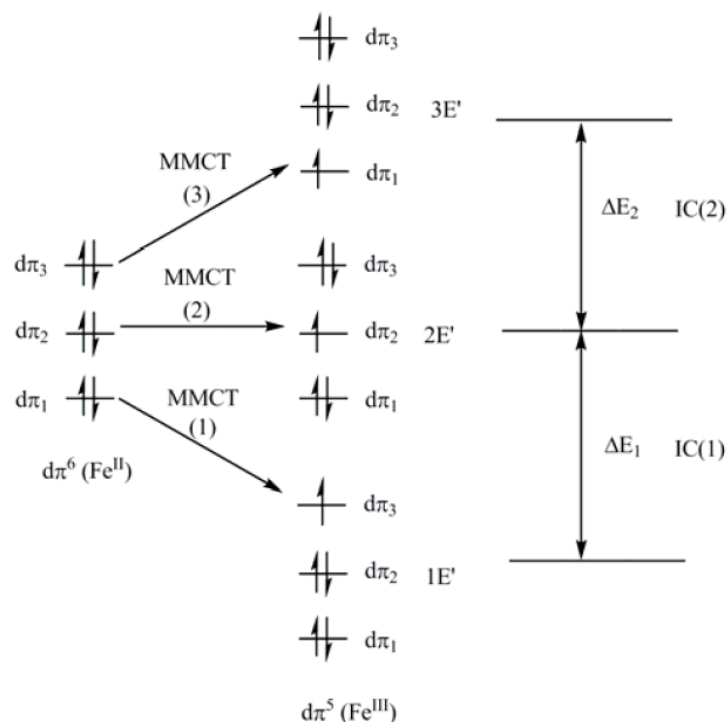


Fig. 3. MMCT and IC transition of coupled bimetallic $d\pi^6$ - $d\pi^5$ compounds^[48]

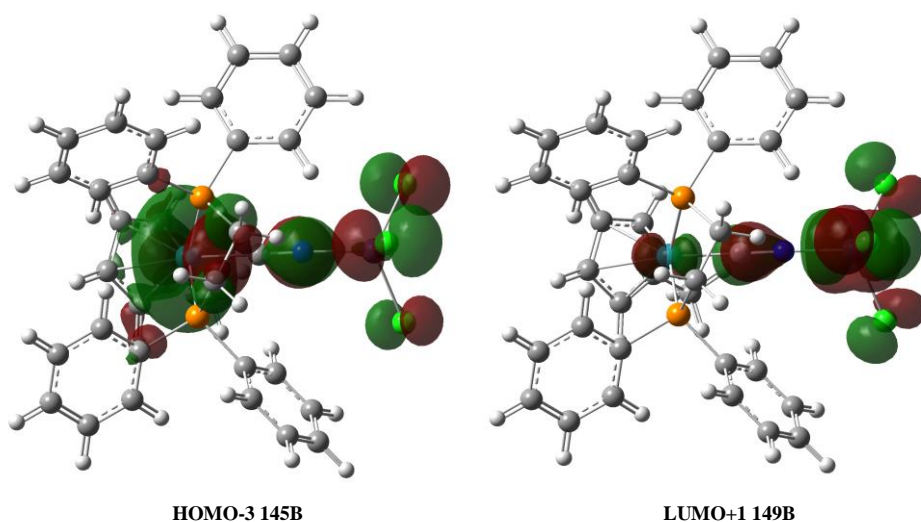
3.4 DFT/TDDFT calculations

The DFT/TDDFT calculations were done at the B3LYP/LANL2DZ level using Gaussian 03 program package^[46], and its result can be exploited to study the mechanism of MMCT properties. From Table 4, it is concluded that the major spin densities of all mixed-valence complexes are distributed over the FeCl_3 moiety, which confirms these complexes belong to the Class II MV compounds. According to spin densities, the redox sites of FeCl_3 moiety in all complexes are not much different, while the potential of Fe center on the donor site is larger than that of Ru. It can also explain the phenomenon of the lower $\nu(\text{CN})$ of complex **3** than that of complexes **4** and **5**. Compared the theoretical calculation of all complexes with experimental results, the calculated electronic transition bands are in good agreement with the experimental transition (Table 3). For

complex **1**, the calculated absorption band appears at 519.90 nm in the NIR regions, which accords with the experimental result (500 nm). The plot of molecular orbitals displays distinctly that the orientation of some electrons flow is from the MeCpRu fragment to the FeCl_3 fragment (Fig. 4) and it proceeds predominately with the molecular orbital HOMO-3 (145B) \rightarrow LUMO+1 (149B) transition. For the other complexes, the MMCT from Ru^{II} or Fe^{II} to Fe^{III} are predominated with HOMO-2 (178B) \rightarrow LUMO+1 (182B) for **2**, HOMO-1 (162B) \rightarrow LUMO (164B) for **3**, HOMO-1 (162B) \rightarrow LUMO (164B) and HOMO (163B) \rightarrow LUMO+1 (165B) for **4**, and HOMO-2 (194B) \rightarrow LUMO+1 (198B) for **5**, as shown in Figs. 5~8, respectively. According to the Robin and Day's classification^[47], these complexes can be attributed to the typical Class II mixed-valence compounds.

Table 4. Mulliken Spin Densities of Mixed-valence Species

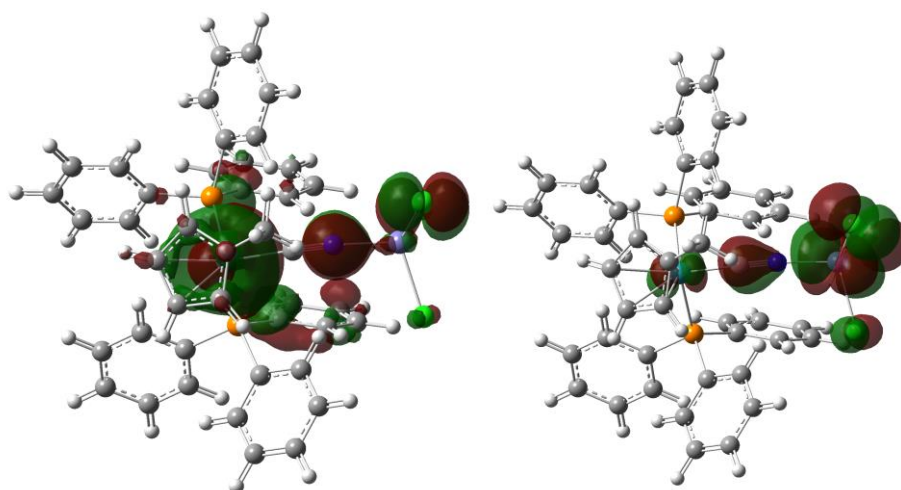
Complex	Ru/Fe	Fe
1	0.048950	3.699288
2	0.045071	3.709902
3	0.102101	3.771728
4	0.053790	3.707974
5	0.059390	3.686879



HOMO-3 145B

LUMO+1 149B

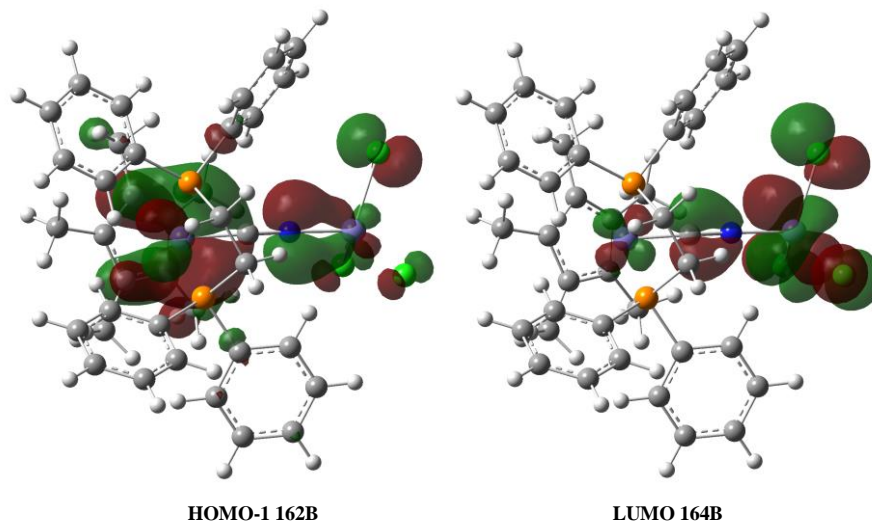
Fig. 4. Molecular orbital diagrams of HOMO-3 (145B), and LUMO+1 (149B) for 1.
The isosurface value is 0.02 au.



HOMO-2 178B

LUMO+1 182B

Fig. 5. Molecular orbital diagrams of HOMO-2 (178B) and LUMO+1 (182B) for 2.
The isosurface value is 0.02 au.



HOMO-1 162B

LUMO 164B

Fig. 6. Molecular orbital diagrams of HOMO-1 (162B) and LUMO (164B) for 3.
The isosurface value is 0.02 au.

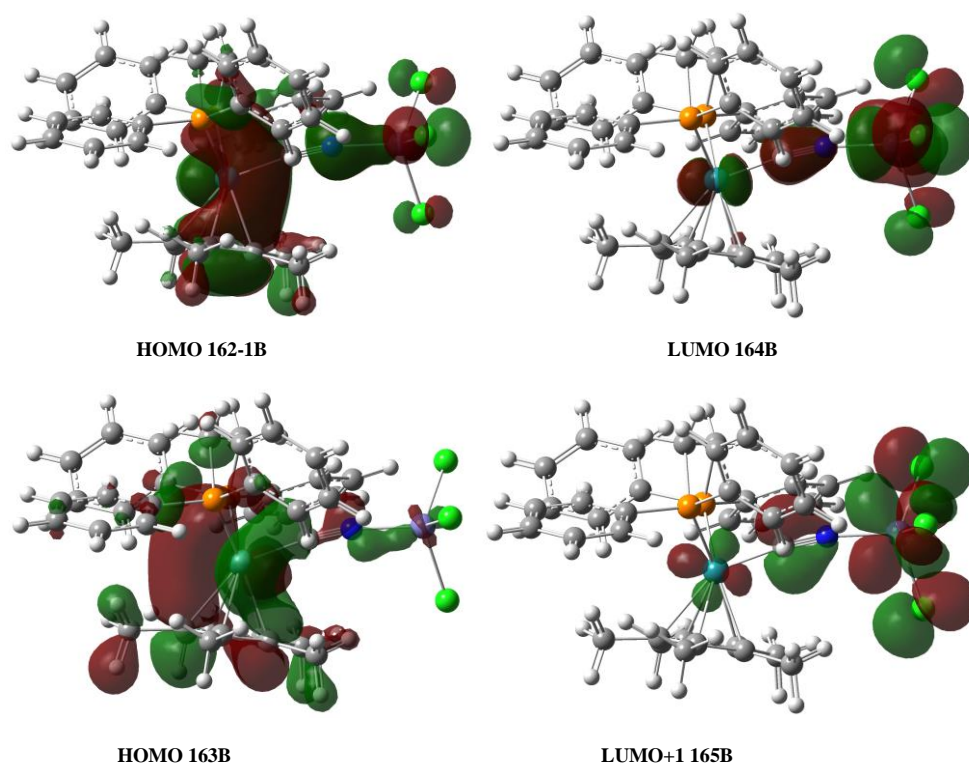


Fig. 7. Molecular orbital diagrams of HOMO-1 (162B), HOMO (163B), LUMO (164B) and LUMO+1 (165B) for **4**. The isosurface value is 0.02 au.

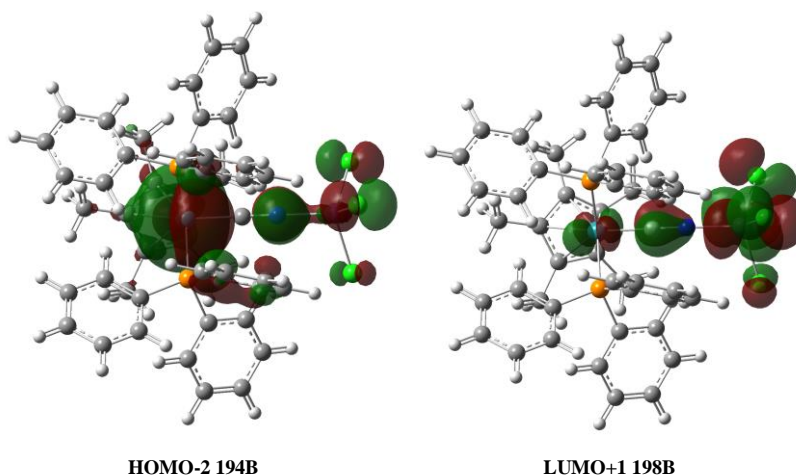


Fig. 8. Molecular orbital diagrams of HOMO-2 (194B) and LUMO+1 (198B) for **5**. The isosurface value is 0.02 au.

4 CONCLUSION

In summary, a new family of binuclear complexes, $L_1L_2M-CN-FeCl_3$ ($L_1 = dppe$ or $(PPh_3)_2$, $L_2 = Cp$ or Cp^* , $M = Ru$ or Fe) have been synthesized and characterized by single-crystal X-ray diffraction structural analyses, IR spectra, UV-Vis spectroscopy and the DFT/TDDFT calculation thoroughly. The electronic absorptions of these complexes show the presence of MMCT properties between $Ru^{II}(Fe^{II})$ and Fe^{III} ions, strongly supported by the theoretical calcula-

tions. Compared to complex **4**, the MMCT absorption band of complex **3** ($L_1L_2Fe-CN-FeCl_3$) is red-shift. From the electronic spectra, the sequence of the MMCT absorption bands from high-energy to low energy is **1** (500 nm) > **4** (536 nm) > **2** (542 nm) > **5** (580 nm) and **4** (536 nm) > **3** (760 nm). In a word, this work suggests that the stronger electron-donating ligand or metal at donor site is the lower energy the MMCT needs. Furthermore, the investigations indicate that the unsymmetrical MV complexes belong to the Class II systems according to the Robin and Day's classification.

REFERENCES

- (1) Miyasaka, H.; Matsumoto, N.; Ōkawa, H.; Re, N.; Gallo, E.; Floriani, C. Complexes derived from the reaction of manganese(III) Schiff base complexes and hexacyanoferrate(III): syntheses, multidimensional network structures, and magnetic properties. *J. Am. Chem. Soc.* **1996**, 118, 981–994.
- (2) Ohba, M.; Ōkawa, H.; Ito, T.; Ohto, A. A two-dimensional bimetallic assembly, $[\text{Ni}(\text{pn})_2]_2[\text{Fe}(\text{CN})_6]\text{ClO}_4 \cdot 2\text{H}_2\text{O}$, with a square structure. *J. Chem. Soc., Chem. Commun.* **1995**, 15, 1545–1546.
- (3) Harris, T. D.; Coulon, C.; Clérac, R.; Long, J. R. Record ferromagnetic exchange through cyanide and elucidation of the magnetic phase diagram for a $\text{Cu}^{\text{II}}\text{Re}^{\text{IV}}(\text{CN})_2$ chain compound. *J. Am. Chem. Soc.* **2010**, 133, 123–130.
- (4) Bruce, M. I.; Costuas, K.; Davin, T.; Ellis, B. G.; Halet, J. F.; Lapinte, C.; Low, P. J.; Smith, M. E.; Skelton, B. W.; Toupet, L. Iron versus ruthenium: dramatic changes in electronic structure result from replacement of one Fe by Ru in $[\{\text{Cp}^*(\text{dppe})\text{Fe}\}-\text{CC}-\text{CC}-\{\text{Fe}(\text{dppe})\text{Cp}^*\}]^{n+}$ ($n = 0, 1, 2$). *Organometallics* **2005**, 24, 3864–3881.
- (5) Ma, X.; Hu, S. M.; Tan, C. H.; Zhang, Y. F.; Zhang, X. D.; Sheng, T. L.; Wu, X. T. From antiferromagnetic to ferromagnetic interaction in cyanido-bridged Fe(III)–Ru(II)–Fe(III) complexes by change of the central diamagnetic cyanido-metal geometry. *Inorg. Chem.* **2013**, 52, 11343–11350.
- (6) Wang, X. Y.; Avendaño, C.; Dunbar, K. R. Molecular magnetic materials based on 4d and 5d transition metals. *Chem. Soc. Rev.* **2011**, 40, 3213–3238.
- (7) Metz, J.; Hanack, M. Synthesis, characterization, and conductivity of (μ -cyano)(phthalocyaninato) cobalt(III). *J. Am. Chem. Soc.* **1983**, 105, 828–830.
- (8) Bignozzi, C. A.; Argazzi, R.; Garcia, C. G.; Scandola, F.; Schoonover, J. R.; Meyer, T. J. Long-range energy transfer in oligomeric metal complex assemblies. *J. Am. Chem. Soc.* **1992**, 114, 8727–8729.
- (9) Endicott, J. F.; Chen, Y. J. Electronic coupling between metal ions in cyanide-bridged ground state and excited state mixed valence complexes. *Coordin. Chem. Rev.* **2013**, 257, 1676–1698.
- (10) Lin, J. L.; Tsai, C. N.; Huang, S. Y.; Endicott, J. F.; Chen, Y. J.; Chen, H. Y. Nearest-and next-nearest-neighbor Ru(II)/Ru(III) electronic coupling in cyanide-bridged tetra-ruthenium square complexes. *Inorg. Chem.* **2011**, 50, 8274–8280.
- (11) Alborés, P.; Rossi, M. B.; Baraldo, L. M.; Slep, L. D. Donor-acceptor interactions and electron transfer in cyano-bridged trinuclear compounds. *Inorg. Chem.* **2006**, 45, 10595–10604.
- (12) Sheng, T.; Vahrenkamp, H. Long range metal-metal interactions along Fe–NC–Ru–CN–Fe chains. *Eur. J. Inorg. Chem.* **2004**, 1198–1203.
- (13) Low, P. J. Twists and turns: studies of the complexes and properties of bimetallic complexes featuring phenylene ethynylene and related bridging ligands. *Coordin. Chem. Rev.* **2013**, 257, 1507–1532.
- (14) Chisholm, M. H. Mixed valency and metal-metal quadruple bonds. *Coordin. Chem. Rev.* **2013**, 257, 1576–1583.
- (15) Kaim, W.; Lahiri, G. K. Unconventional mixed-valent complexes of ruthenium and osmium. *Angew. Chem. Int. Edit.* **2007**, 46, 1778–1796.
- (16) D'Alessandro, D. M.; Keene, F. R. Intervalence charge transfer (IVCT) in trinuclear and tetranuclear complexes of iron, ruthenium, and osmium. *Chem. Rev.* **2006**, 106, 2270–2298.
- (17) Oviedo, P. S.; Pieslinger, G. E.; Cadranell, A.; Baraldo, L. M. Exploring the localized to delocalized transition in non-symmetric bimetallic ruthenium polypyridines. *Dalton Trans.* **2017**, 46, 15757–15768.
- (18) Pieslinger, G. E.; Albores, P.; Slep, L. D.; Coe, B. J.; Timpson, C. J.; Baraldo, L. M. Communication between remote moieties in linear Ru–Ru–Ru trimetallic cyanide-bridged complexes. *Inorg. Chem.* **2013**, 52, 2906–2917.
- (19) Ma, X.; Lin, C. S.; Hu, S. M.; Tan, C. H.; Wen, Y. H.; Sheng, T. L.; Wu, X. T. Influence of central metalloligand geometry on electronic communication between metals: syntheses, crystal structures, MMCT properties of isomeric cyanido-bridged Fe_2Ru complexes, and TDDFT calculations. *Chem. Eur. J.* **2014**, 20, 7025–36.
- (20) Hush, N. S. Intervalence-transfer absorption. Part 2. Theoretical considerations and spectroscopic data. *Prog. Inorg. Chem.* **1967**, 391–444.
- (21) Brunschwig, B. S.; Creutz, C.; Sutin, N. Optical transitions of symmetrical mixed-valence systems in the Class II–III transition regime. *Chem. Soc. Rev.* **2002**, 31, 168–184.
- (22) Demadis, K. D.; Hartshorn, C. M.; Meyer, T. J. The localized-to-delocalized transition in mixed-valence chemistry. *Chem. Rev.* **2001**, 101, 2655–2686.
- (23) Cave, R. J.; Newton, M. D. Generalization of the Mulliken-Hush treatment for the calculation of electron transfer matrix elements. *Chem. Phys. Lett.* **1996**, 249, 15–19.
- (24) Marcus, R. A.; Sutin, N. Electron transfers in chemistry and biology. *Biochimica et Biophysica Acta (BBA)-Reviews on Bioenergetics* **1985**, 811,

265–322.

- (25) Adams, C. J.; Connelly, N. G.; Goodwin, N. J.; Hayward, O. D.; Orpen, A. G.; Wood, A. J. Metal-metal charge transfer and solvatochromism in cyanomanganese carbonyl complexes of ruthenium and osmium. *Dalton Trans.* **2006**, 29, 3584–96.
- (26) Pereztejada, P.; Neto-Ponce, P.; Sánchez, F. Salt effects on the electron transfer transition within the binuclear complex $[(\text{NH}_3)_5\text{Ru}^{\text{III}}(\mu\text{-CN})\text{Fe}^{\text{II}}(\text{CN})_5]^-$. *J. Chem. Soc., Dalton Trans.* **2001**, 11, 1686–1691.
- (27) Sánchez-Burgos, F.; Galán, M.; Domínguez, M.; Pe'rez-Tejeda, P. Medium effects on the electron transfer transition within the binuclear complex $[(\text{NH}_3)_5\text{Ru}^{\text{III}}\text{-NC-Ru}^{\text{II}}(\text{CN})_5]$. *New J. Chem.* **1998**, 22, 907–911.
- (28) Rossi, M. B.; Alborés, P.; Baraldo, L. M. Exploring the properties of mixed valence cyanide bridged dinuclear complexes: solvent stabilization of electronic isomers. *Inorg. Chim. Acta* **2011**, 374, 334–340.
- (29) Neto-Ponce, P.; Sánchez, F.; Pérez, F.; García-Santana, A.; Pérez-Tejeda, P. Salt, solvent, and micellar effects on the intervalence transition within the binuclear complex pentaammineruthenium(III)(μ -cyano)pentacyanoiron(II). An estimation of rate constant from static (optical and electrochemical) data. *Langmuir* **2001**, 17, 980–987.
- (30) Ma, X.; Lin, C. S.; Zhu, X. Q.; Hu, S. M.; Sheng, T. L.; Wu, X. T. An unusually delocalized mixed-valence state of a cyanidometal-bridged compound induced by thermal electron transfer. *Angew. Chem. Int. Edit.* **2017**, 56, 1605–1609.
- (31) Su, S. D.; Zhu, X. Q.; Wen, Y. H.; Zhang, L. T.; Yang, Y. Y.; Lin, C. S.; Wu, X. T.; Sheng, T. L. A diruthenium-based mixed spin complex Ru_2^{5+} ($S = 1/2$)– CN-Ru_2^{5+} ($S = 3/2$). *Angew. Chem. Int. Edit.* **2019**, 58, 15344–15348.
- (32) Sheldrick, G. M. Crystal structure refinement with SHELXL. *Acta Crystallogr. C Struct. Chem.* **2015**, 71, 3–8.
- (33) Sheldrick, G. M. A short history of SHELX. *Acta Crystallogr. Sect. A* **2008**, 64, 112–122.
- (34) Dolomanov, O. V.; Bourhis, L. J.; Gildea, R. J.; Howard, J. A. K.; Puschmann, H. OLEX₂: a complete structure solution, refinement and analysis program. *J. Appl. Cryst.* **2009**, 42, 339–341.
- (35) Li, S. H.; Liu, Y.; Yang, Y. Y.; Zhang, Y. X.; Xu, Q. D.; Hu, S. M.; Wu, X. T.; Sheng, T. L. Syntheses, crystal structures and MMCT properties of cyanide-bridged binuclear Ru–Fe complexes. *Polyhedron* **2019**, 114109–114109.
- (36) Roger, C.; Hamon, P.; Toupet, L.; Rabaa, H.; Saillard, J. Y.; Hamon, J. R.; Lapinte, C. Halo and alkyl (pentamethylcyclopentadienyl)(1,2-bis(diphenylphosphino)ethane)iron(III) 17-electron complexes: synthesis, NMR and magnetic-properties, and EHMO calculations. *Organometallics* **1991**, 10, 1045–1054.
- (37) Bruce, M. I.; Ellis, B. G.; Low, P. J.; Skelton, B. W.; White, A. H. Syntheses, structures, and spectro-electrochemistry of $\{\text{Cp}^*(\text{PP})\text{Ru}\}\text{C}\equiv\text{CC}\equiv\text{C}\{\text{Ru}(\text{PP})\text{Cp}^*\}$ (PP = dpmm, dppe) and their mono-and dications. *Organometallics* **2003**, 22, 3184–3198.
- (38) Yang, Y. Y.; Zhu, X. Q.; Hu, S. M.; Su, S. D.; Zhang, L. T.; Wen, Y. H.; Wu, X. T.; Sheng, T. L. Different degrees of electron delocalization in mixed valence Ru–Ru–Ru compounds by cyanido-/isocyanido-bridge isomerism. *Angew. Chem. Int. Edit.* **2018**, 57, 14046–14050.
- (39) Morandini, F.; Dondana, A.; Munari, I.; Pilloni, G.; Consiglio, G.; Sironi, A.; Moret, M. Pentamethylcyclopentadienyl ruthenium(II) complexes containing chiral diphosphines: synthesis, characterisation and electrochemical behaviour. X-ray structure of $(\eta^5\text{-C}_5\text{Me}_5)\text{Ru}\{(\text{S,S})\text{-Ph}_2\text{PCH}(\text{CH}_3)\text{CH}(\text{CH}_3)\text{PPh}_2\}\text{Cl}$. *Inorg. Chim. Acta* **1998**, 282, 163–172.
- (40) Zhang, L. T.; Zhu, X. Q.; Su, S. D.; Yang, Y. Y.; Hu, S. M.; Wen, Y. H.; Wu, X. T.; Sheng, T. L. Influence of the substitution of the ligand on MMCT properties of mixed valence heterometallic cyanido-bridged Ru–Fe complexes. *Cryst. Growth Des.* **2018**, 18, 3674–3682.
- (41) Zhang, L. T.; Zhu, X. Q.; Hu, S. M.; Zhang, Y. X.; Su, S. D.; Yang, Y. Y.; Wu, X. T.; Sheng, T. L. Influence of ligand substitution at the donor and acceptor center on MMCT in a cyanide-bridged mixed-valence system. *Dalton Trans.* **2019**, 48, 7809–7816.
- (42) Sheng, T.; Vahrenkamp, H. In metal-metal charge transfer in LnM-CN-FeCl_3 complexes. *An. Asoc. Quím. Argent.* **2004**, 17–27.
- (43) Zhu, N.; Vahrenkamp, H. Synthesis, redox chemistry, and mixed-valence phenomena of cyanide-bridged dinuclear organometallic complexes. *Chem. Ber.* **1997**, 130, 1241–1252.
- (44) Bignozzi, C. A.; Roffia, S.; Scandola, F. Intervalence transfer in cyano-bridged bi- and trinuclear ruthenium complexes. *J. Am. Chem. Soc.* **1985**, 107, 1644–1651.
- (45) Richardson, D. E. T. H. Electronic interactions in mixed-valence molecules as mediated by organic bridging groups. *J. Am. Chem. Soc.* **1983**, 105, 40–51.
- (46) Frisch, M. J.; Trucks, G. W.; Schlegel, H. B.; Scuseria, G. E.; Robb, M. A.; Cheeseman, J. R.; Scalmani, G.; Barone, V.; Mennucci, B.; Petersson, G. A.; Nakatsuji, H.; Caricato, M.; Li, X.; Hratchian, H. P.; Izmaylov, A. F.; Bloino, J.; Zheng, G.; Sonnenberg, J. L.; Hada, M.; Ehara, M.; Toyota, K.; Fukuda, R.; Hasegawa, J.; Ishida, M.; Nakajima, T.; Honda, Y.; Kitao, O.; Nakai, H.; Vreven, T.; Montgomery, Jr. J. A.; Peralta, J. E.; Ogliaro, F.

- Bearpark, M.; Heyd, J. J.; Brothers, E.; Kudin, K. N.; Staroverov, V. N.; Keith, T.; Kobayashi, R.; Normand, J.; Raghavachari, K.; Rendell, A.; Burant, J. C.; Iyengar, S. S.; Tomasi, J.; Cossi, M.; Rega, N.; Millam, J. M.; Klene, M.; Knox, J. E.; Cross, J. B.; Bakken, V.; Adamo, C.; Jaramillo, J.; Gomperts, R.; Stratmann, R. E.; Yazyev, O.; Austin, A. J.; Cammi, R.; Pomelli, C.; Ochterski, J. W.; Martin, R. L.; Morokuma, K.; Zakrzewski, V. G.; Voth, G. A.; Salvador, P.; Dannenberg, J. J.; Dapprich, S.; Daniels, A. D.; Farkas, O.; Foresman, J. B.; Ortiz, J. V.; Cioslowski, J.; Fox, D. J. Gaussian, Inc., Wallingford CT **2013**.
- (47) Robin, M. B.; Day, P. Mixed valence chemistry-a survey and classification. *Advances in Inorganic Chemistry and Radiochemistry* **1968**, 10, 247–422.
- (48) Ma, X. *Designed Synthesis, MMCT and Magnetic Properties of a Series of Cyanide-bridged Organometallic Complexes*. Doctor Thesis, Fujian Institute of Research on the Structure of Matter, Chinese Academy of Sciences **2012**, p71–72.